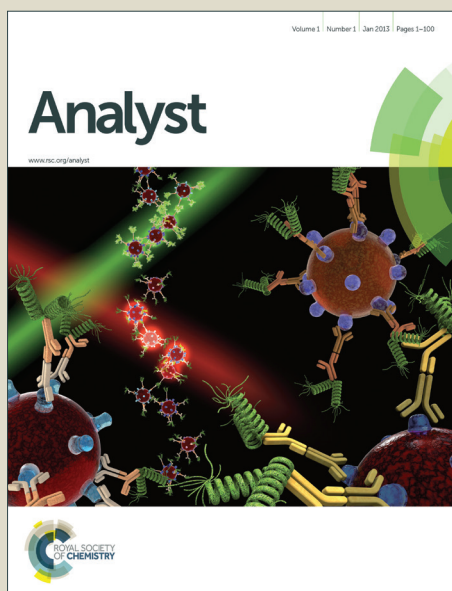


Analyst

Accepted Manuscript



This is an *Accepted Manuscript*, which has been through the Royal Society of Chemistry peer review process and has been accepted for publication.

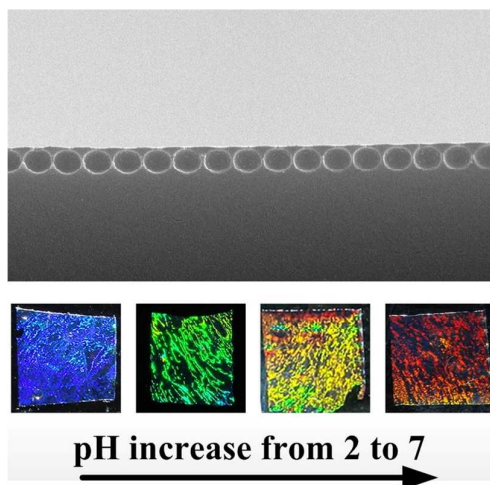
Accepted Manuscripts are published online shortly after acceptance, before technical editing, formatting and proof reading. Using this free service, authors can make their results available to the community, in citable form, before we publish the edited article. We will replace this *Accepted Manuscript* with the edited and formatted *Advance Article* as soon as it is available.

You can find more information about *Accepted Manuscripts* in the [Information for Authors](#).

Please note that technical editing may introduce minor changes to the text and/or graphics, which may alter content. The journal's standard [Terms & Conditions](#) and the [Ethical guidelines](#) still apply. In no event shall the Royal Society of Chemistry be held responsible for any errors or omissions in this *Accepted Manuscript* or any consequences arising from the use of any information it contains.

Graphical abstract

Two dimensional (2D) inverse opal hydrogels with well-ordered macroporous monolayer on the surface are prepared by polymerization of hydrogel monomers on 2D array templates and shows prompt response to pH stimuli by the change of diffraction color.



ARTICLE

Two dimensional inverse opal hydrogel for pH sensing

Cite this: DOI: 10.1039/x0xx00000x

Fei Xue, Zihui Meng*, Fenglian Qi, Min Xue*, Fengyan Wang, Wei Chen, and Zequn Yan

Received 00th January 2012,

Accepted 00th January 2012

DOI: 10.1039/x0xx00000x

www.rsc.org/

A novel hydrogel film with a highly ordered macropore monolayer on its surface was prepared by templated photo-polymerization of hydrogel monomers on a two-dimensional (2D) polystyrene colloidal array. The 2D inverse opal hydrogel has prominent advantages over traditional three-dimensional (3D) inverse opal hydrogels. First, the formation of 2D array template through self-assembly method is much faster and simpler. Second, the stable ordering structure of the 2D array template makes it easier to introduce polymerization solution into the template. Third, a simple measurement, Debye diffraction ring is utilized to characterize the neighboring pore spacing of the 2D inverse opal hydrogel. Acrylic acid was copolymerized into the hydrogel, thus the hydrogel responded to pH through volume change which resulted from the formation of the Donnan potential. The 2D inverse opal hydrogel showed that the neighboring pore spacing increased about 150 nm and diffracted color red-shifted from blue to red as the pH increased from pH 2 to 7. In addition, the pH response kinetics and ionic strength effect of this 2D mesoporous polymer film were also investigated.

Introduction

There is great interest for the development of highly ordered porous functional structures through colloidal crystal templating in the fields of optics, chemical sensing, and microfluidics.¹⁻⁵ Because the periodicity of the colloidal crystal template is on the order of hundreds of nanometers, the resulting highly ordered porous (inverse opal) materials interact with visible light, leading to optical diffraction following Bragg diffraction.⁶⁻⁸ Inverse opal hydrogel structures are especially attractive because hydrogel may swell or shrink in aqueous solution upon physical and chemical stimuli by changing their dimensions, which leads to spectral shifts in the Bragg diffraction wavelength and structural color change. Most of the reported inverse opal responsive hydrogels use three-dimensional (3D) colloidal arrays as templates.⁹⁻¹⁴ However, for the successful formation of these inverse opal sensing materials, each fabrication is strongly dependent on the formation of a well-ordered 3D colloidal crystal template and carefully experimental process control. Unfortunately, the self-assembly of 3D colloidal crystal is time-consuming (days to weeks). In addition, the ordering of the 3D colloidal crystal templates is likely to be damaged during the introduction of polymerization precursor. Thus, it is desirable to develop new

inverse opal hydrogel sensing materials which are easy to prepare.

Herein, we use two-dimensional (2D) colloidal array as template to prepare inverse opal hydrogel films. The preparation of 2D colloidal array is much simpler and faster than the formation of 3D colloidal array template.^{15,16} After photo-polymerization of 2-hydroxyethyl methacrylate-co-acrylic acid (HEMA-AA) hydrogel on the stable 2D array followed by etching the 2D array template, a 2D inverse opal hydrogel film was obtained. The resultant 2D inverse opal hydrogel film has a monolayer with highly ordered pores on its surface which shows strong optical diffraction following Bragg diffraction law that can be visually observed. Moreover, the 2D inverse opal spacing (neighboring pore spacing) can be easily measured by monitoring the forward 2D inverse opal diffraction that forms a Debye diffraction ring. Due to carboxyl group in the hydrogel network, the 2D inverse opal hydrogel shows pH-sensitive property by changing its volume which induces the diffraction shift of the 2D inverse opal. Finally, the pH response kinetics and ionic strength effect of this 2D mesoporous hydrogel film was investigated. Generally, the fast template preparation, stable array ordering, and simple diffraction characterization make the 2D inverse opal hydrogel an

important component in the family of inverse opal hydrogel sensing materials.

Experimental section

Materials

Styrene was purchased from Sigma. Acrylic acid (AA), KH_2PO_4 , HCl (37%), KCl, and 1-propanol were obtained from Aladdin Co. Ltd. Potassium persulfate, dichloromethane, 2-hydroxyethyl methacrylate (HEMA), 2,2-diethoxyacetophenone (DEAP), ethyleneglycol dimethacrylate (EDMA), NaOH were purchased from Acros Organics and used as received. Deionized water (Aquapro) was used for the experiment.

Preparation of 2D inverse opal hydrogels

Figure 1 illustrates the fabrication of 2D inverse opal hydrogel films for pH sensing, including the preparation of the 2D colloidal array templates, photo-polymerization of the poly (HEMA-AA) hydrogel on the 2D array, and removing of 2D array template.

Polystyrene (PS) particles of ~ 590 nm diameter were synthesized according to a previous method.¹⁷ The PS dispersion concentration of 20 wt % in water and 1-propanol were mixed at a ratio of 3:1 in volume. 20 μL PS suspension was then assemble into a hexagonal close-packed 2D array at the air/water interface in a 10 cm diameter glass dish according to a reported method (Figure 1a).¹⁵ This 2D array monolayer was then transferred onto a glass slide (20 \times 20 mm) (Figure 1b,c).

2.33 mL HEMA, AA (5 mol-%, 2.5 mol-% or 0 mol-% vs. HEMA), 23.7 μL EDMA, 58.9 μL DEAP and 1.925 mL H_2O were mixed and deoxygenated by N_2 bubbling for 10 min. 50 μL of the polymerization solution was layered carefully on the 2D array on a glass slide (20 \times 20 mm) followed by covering with another glass slide (20 \times 20 mm) to form a “sandwich” system (Figure 1d). After photo-polymerization by UV light for 2 h, the 2D array monolayer was embedded in the hydrogel film (Figure 1e). The hydrogel film with 2D array inside was separated with glass slides and was immersed into dichloromethane overnight to remove the PS particles. After the removal of PS particles, a visibly opalescent inverse 2D opal hydrogel film was formed and washed with large amount of pure water and was stored in phosphate buffer (pH2, 0.1 M) (Figure 1f).

Characterizations

The 2D array and resultant 2D inverse opal hydrogel were characterized using SEM (Quanta FEG 250, FEI) after sputter-coating a layer of gold. The Debye diffraction ring was utilized to characterize the adjacent pore spacing of the 2D inverse opal hydrogel. Typically, a violet laser pointer (405 nm) was illuminated on the 2D inverse opal hydrogel at a normal angle. At normal incidence, the diffracted light on the screen perpendicular to the laser reflects the 2D pore spacing and ordering by showing a ring. The neighboring pore spacing, d , was calculated through the modified diffraction equation using

the ring diameter D , and the distance of the screen to the 2D inverse opal hydrogel sample h .

The 2D inverse opal hydrogel films were cut into 8 mm \times 8 mm pieces for the sensing measurement. The pH dependent Debye diffraction ring measurements were performed on the hydrogel placed in a glass Petri dish filled with buffer solutions of different pH. The phosphate buffers of various pH were prepared by mixing different volumes of 0.1M KH_2PO_4 , 0.1M HCl, 0.1M NaOH. The pH measurement was performed using a pH meter (PC 700, Eutech) at ambient temperature. The photographs of the hydrogel were taken using a digital camera at an angle of $\sim 30^\circ$ between the light source/camera and the 2D inverse opal hydrogel normal. The 2D inverse opal hydrogel films were placed on a silver mirror.

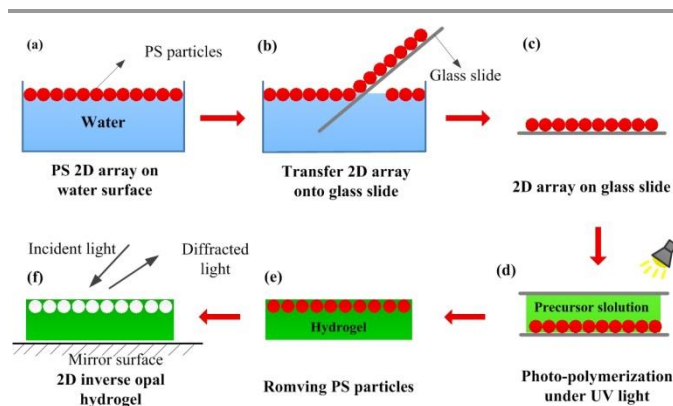


Figure 1. Schematic illustration of experimental procedures.

Results and discussion

Preparation of 2D inverse opal hydrogel films

Formation of 2D colloidal array on water surface is a fast self-assembly process. In this research, when the suspension of PS particles were added to the water surface, PS particles spread rapidly on water surface and self-assembled into a close-packed hexagonal 2D array very quickly. It took less than 1 min to form a well-ordered 2D array with an area of about 75 cm^2 . The 2D array monolayer could be simply transferred to a glass slide by picking up the 2D array by glass slide, as shown in Figure 1b. The ordering of the hexagonal 2D array was maintained well on glass slide during transferring the 2D array from water surface onto glass slide, as shown in the †ESI. The well-ordered close-packed 2D array monolayers were used as templates to prepare 2D inverse opal hydrogel.

Traditional inverse opals are usually fabricated based on 3D colloidal array templates which are generally formed by self-assembly methods. It is known that self-assembly of 3D colloidal array is very slow (days or even weeks), and the experimental conditions, such as the evaporation rate of particle suspension, the concentration of colloidal particles, etc., must be very carefully controlled. Compared with the time consuming and sophisticated fabrication of 3D array, the 2D array monolayer has prominent advantage of fast and simple preparation.

Because the 2D array monolayer has a characteristic spacing of the order of hundreds of nanometers, the resulting structure interacts strongly with visible light, leading to an optical diffraction that follows: $m\lambda = \sqrt{3}d\sin\theta$, where m is the diffraction order, λ is the diffracted wavelength, d is the 2D array particle spacing, and θ is the angle of the light relative to the normal of the 2D array.¹⁶ We controlled θ and d to achieve diffraction in the visible region. 2D array monolayers show strong forward diffraction. In this research, using a reflective mirror, the bright blue back diffracted color of 590 nm PS 2D array could be observed after illuminating the array with a flashlight at an angle of $\sim 30^\circ$ between the light source/camera and the 2D array normal as shown in the †ESI.

Infiltration of polymerization precursor into 3D colloidal array voids needs to be very carefully controlled in order to avoid the damage of the ordering. However, the 2D array monolayer of PS particles attached firmly on the surface of glass slide, and the ordering of the 2D array would not collapse even the glass slide was dipped into water for several times back and forth. Thus, the stable array is a perfect template for the fabrication of highly ordered porous materials. The polymerization solution was simply added on 2D array on glass slide and covered with another glass slide to form a “sandwich” system (Figure 1d). After polymerization and removing the 2D array template, 2D inverse opal hydrogel film was prepared. Figure 2a presents the SEM morphology of the 2D inverse opal hydrogel. We can observe well-ordered pores on the hydrogel surface which demonstrates that 2D array ordering was not damaged during the processing. The persistence of the periodic structure suggests that the hydrogel is mechanically robust. Figure 2b shows the cross section of the 2D inverse opal hydrogel exhibiting ordered monolayer pores on the hydrogel surface. Back diffracted bright blue color (Figure 2c) was observed from the 2D inverse opal hydrogel by putting a mirror under the hydrogel.

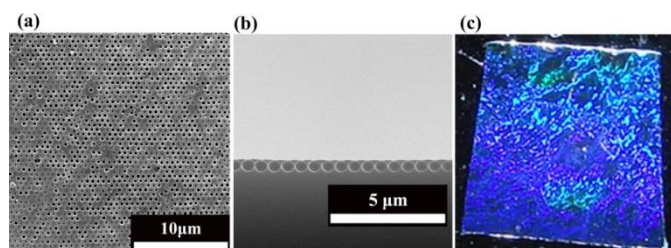


Figure 2. SEM of (a) 2D inverse opal hydrogel and (b) the cross section of 2D inverse opal hydrogel showing monolayer macropore on hydrogel surface. (c) Diffracted color of 2D inverse opal hydrogel.

Characterization of the 2D inverse opal diffraction

The diffraction of certain light of 3D inverse opal hydrogels is mainly utilized to characterize the hydrogel volume response. Thus, spectrometric devices are always used to monitoring the diffracted wavelength shift of the inverse opal hydrogel upon the response to stimulus. However, the spectrometric devices are expensive and complicated to use. For the 2D inverse opal

sensing, we can simplify the detection by detecting the Debye diffraction ring. As shown in Figure 3a, at normal monochromatic incidence, the forward diffracted light of the 2D array monolayer forms a ring on a screen. The Debye diffraction of the 2D array follows: $\sin\alpha = 2\lambda/\sqrt{3}d$, where α is the forward diffraction angle of the Debye diffraction, λ is the incident wavelength, and d is the adjacent particle spacing.¹⁸ For 2D inverse opal sample, d refers to the adjacent pore spacing. The forward diffraction angle, α , can be obtained from $\alpha = \tan^{-1}(D/2h)$, where h is the distance between 2D array and the screen, D is the Debye diffraction ring diameter. Therefore, the particle spacing of 2D array and the pore spacing of 2D inverse opal could be easily determined by measuring the Debye ring diameter D . Figure 3b shows the experimental setup to monitor the diffraction ring diameter in this research. For 2D inverse opal hydrogel characterization, the volumetric change of the hydrogel leads to the change of adjacent pore spacing of the 2D inverse opal which induces the Debye diffraction ring diameter change. Compared with the measurement of diffraction wavelength, this method is much easier to operate. Sometimes, the diffraction wavelength cannot be measured by a visible wavelength spectrometer if the wavelength is in the invisible region. However, we can still detect the 2D inverse hydrogel neighboring pore spacing by monitoring the Debye diffraction ring. In the following research, Debye diffraction ring was utilized to characterize the responses of the 2D inverse opal hydrogel.

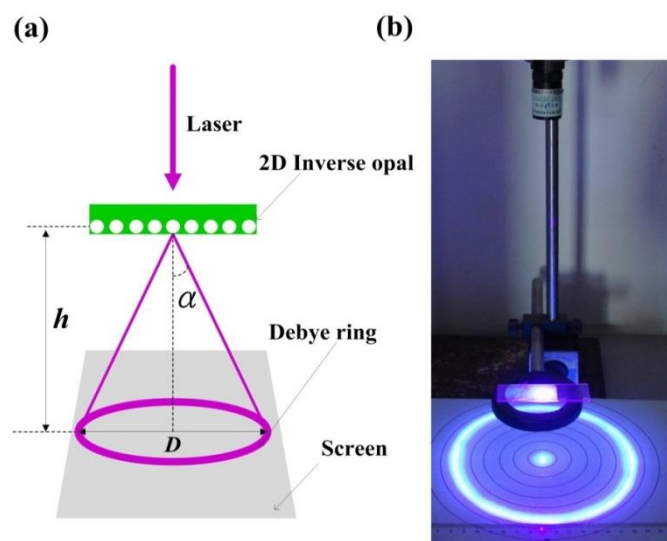


Figure 3. (a) Schematic illustration of the Debye diffraction ring pattern. (b) Photograph showing the experimental setup to measure the Debye diffraction ring of 2D inverse opal hydrogel under a 405 nm incidence laser wavelength.

pH response of the 2D inverse opal hydrogel film

A mixture of HEMA, AA and EDMA was selected as building block, because hydrogels with carboxyl groups have volume change in response to pH due to the dissociation of the carboxyl group which leads to Donnan potential which creates an osmotic pressure that swells the hydrogel.^{20,21} As pH

increase, more and more carboxyl groups deprotonate which increase the hydrogel charge intensity. The charged hydrogel immobilize counter ions inside the hydrogel resulting in an osmotic pressure, which swells the hydrogel. In this research, the carboxyl groups in the hydrogel are from AA monomers. Different concentrations of AA (5 mol-%, 2.5 mol-%, and 0 mol-% vs. HEMA) were chosen to determine its effects to pH sensitivity. The 2D inverse opal poly HEMA-AA hydrogel films were synthesized with the compositions listed in Table 1. The pH-dependent optical diffraction of the monolayer mesoporous hydrogel films was characterized using Debye diffraction ring. Figure 4a shows the pH response of the 2D inverse opal hydrogel pore spacing as pH increase and decrease in phosphate buffer. When $\text{pH} \leq 4$, most of the carboxyl groups were protonated, and the 5% AA hydrogel film was in its original contracting state, and the 2D inverse opal hydrogel film had 595 nm pore spacing calculated using the Debye diffraction equation which is close to the diameter of PS particles. As the pH increased, more and more charged carboxyl group resulted in an osmotic pressure which swelled the hydrogel. Thus, the pore spacing steadily increased until it reached 745 nm at pH 7. About 150 nm pore spacing increase was occurred. Although the pK_a (K_a is the dissociation constant of acid) of AA is 4.25 at 25 °C, the actual pK_a of AA within co-polymeric hydrogel is reported to be slightly higher due to an electrostatic interaction of adjacent AA units.¹⁹ Thus, in this research, it is noted in Figure 4a that the hydrogel swelled most from pH 5 to pH 6. As pH increased to above 7, the pore spacing increased slightly since most of AA units had already deprotonated at pH8. In comparison, the 2.5% AA hydrogel pore spacing increased from 595 nm to 659 nm at pH 7. Only 64 nm pore spacing increase occurred. A control sample containing only HEMA exhibited a pore spacing increasing of 5 nm, which can be explained by small quantities of acidic impurities in HEMA.

Table 1. Composition of 2D inverse opal hydrogels

Label	Composition				
	HEMA mmol	AA mmol	EDMA mmol	DEAP mmol	Water mL
5% AA	19.2	9.6	0.126	0.293	1.925
2.5% AA	19.2	4.8	0.126	0.293	1.925
Control	19.2	0	0.126	0.293	1.925

When the direction of pH change was reversed, the pore spacing of the AA containing films decreased until the original pore spacing were recovered. Interestingly, an apparent hysteresis was observed in the pore spacing response for increasing and decreasing pH sweeps. The major reason for the hysteresis might be attributed to the low ionic strength to fully re-equilibrate the Donnan potential during pH decrease. Figure 4b shows a typical color change of the 5% AA 2D inverse opal hydrogel films as a function of pH change. As

shown in Figure 4b, the color changes of the 2D inverse opal hydrogel were observed over a large area with pH variation, and the color covered the visible wavelength between pH2-7. As pH increased to above 7, the pore spacing of the hydrogel continued to swell slightly, but the corresponding color change was not recognizable since red color is located at the long wavelength edge of the visible spectrum.

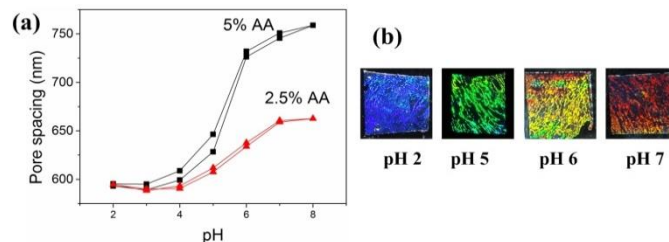


Figure 4. (a) pH-dependent pore spacing change of the 2D inverse opal hydrogel via pH increase and decrease. (b) Diffraction color change of the 5% AA 2D inverse opal hydrogel in response to pH.

The pH-sensitive hydrogel film with a monolayer pores is thin (~12.5 μm). As a result, we measured the response time during the pH increase (from pH 5 to pH 6) and decrease (from pH 6 to pH 5) as well. For the pH increase experiment, the 5% AA 2D inverse opal hydrogel in the pH5 buffer was transferred to a fresh pH6 buffer. The pH decrease experiment was done in the same manner by transferring the hydrogel to a fresh pH5 buffer. The time dependent pore spacing d for pH increase is shown in Figure 5a. Increasing pH from 5 to 6 caused pore spacing to increase slowly from 629 nm to 645 nm within 90 s, followed by a fast increase to equilibration at 726 nm within 500 s. This kinetics of swelling for a charged polyelectrolyte network during pH change may be modelled as a hindered diffusion-limited process which is similar as reported literature.¹⁴ In addition to the pH increase, the response time for the pH decrease (pH 6 to 5) was also monitored. As shown in Figure 5b, after a rapid decrease of pore spacing from 720 nm to 685 nm within 300 s, a slow restoration of d back to 629 nm took place. Shin and coworkers implied that there might be two distinct deswelling mechanisms in the kinetics.²⁰

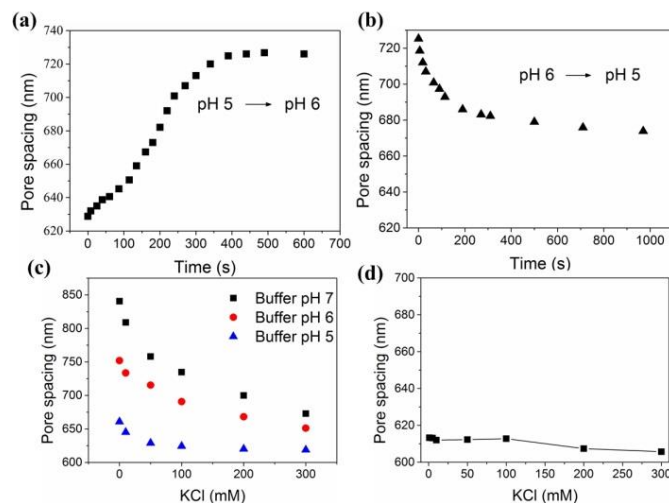


Figure 5. Response kinetics of the 2D inverse opal hydrogel during pH increase (a) and decrease (b) between 5 and 6. Ionic strength dependence of the 2D inverse opal hydrogel pore spacing in phosphate puffer (pH 5,6 and 7, 10 mM) (c) and unbuffered 1mM HCl (d).

The ionic strength dependence of the pH-sensitive 2D inverse opal hydrogel was investigated by varying the KCl concentration in phosphate buffers (pH5, pH6, and pH 7, 10 mM) and an HCl solution (1mM). When the 5% AA hydrogel film was in phosphate buffer (pH5, 10 mM) solutions with increasing the concentration of KCl from 0 to 300 mM, its volumes shrunk, and its pore spacing decreased from 661 to 619 nm (Figure 5c). This is because the hydrogel network is in the swelling state due to Donnan potential at pH5, and higher ionic strength screens the Donnan potential which lead to the shrink of the hydrogel.²¹ Similarly, the hydrogels in phosphate buffer (pH6 and pH7, 10 mM) also shrunk during increasing the KCl concentration from 0 to 300 mM (Figure 5c). When KCl concentration was varied in 1 mM HCl solution, the hydrogel, which was then in neutral state at this acid concentration, exhibited a small pore spacing decrease from 613 nm at 0.1 mM KCl to 606 nm at 300 mM KCl (Figure 5d). The observed shrinking is most likely a result of decrease nonspecific hydrophilic interactions between the hydrogel network and water molecules as KCl concentration increase, also known as the “salting out” effect.²²

Conclusions

In summary, we present a novel responsive hydrogel film with highly ordered monolayer pores on its surface through 2D array templating method. The fast preparation of 2D array template accelerates and simplifies the preparation of inverse opal hydrogel film. Debye diffraction ring diameter is utilized to characterize the 2D inverse opal hydrogel swelling, and could calculate the pore spacing of the monolayer pore on the hydrogel surface. The 2D inverse opal hydrogel exhibits pH-dependent change in pore spacing and the diffracted color shift. Efforts are underway to optimize the diffraction response by changing thickness and chemistry, with a goal of creating colorimetric chemical and biological sensors.

Acknowledgements

This research was supported by NSFC (21375009) and the National Basic Research Program of China (973 program No. 2012CB910603).

Notes and references

School of Chemical Engineering and Environment, Beijing Institute of Technology, Beijing, China 100081

*Corresponding authors: Zihui Meng, E-mail: m_zihui@yahoo.com, Min Xue, Email: minxue@bit.edu.cn

† Electronic Supplementary Information (ESI) available: The SEM image and diffraction color of the 2D colloidal array template. See DOI: 10.1039/b000000x/

- 1 Citations here in the format A. Name, B. Name and C. Name, *Journal Title*, 2000, **35**, 3523; A. Name, B. Name and C. Name, *Journal Title*, 2000, **35**, 3523.
1. P. Jiang, M. J. McFarland, *J. Am. Chem. Soc.*, 2004, **126**, 13778.
2. J. Huang, C. Tao, Q. An, W. Zhang, Y. Wu, X. Li, D. Shen and G. Li, *Chem. Commun.* 2010, **46**, 967.
3. A. Stein, B. E. Wilson and S. G. Rudisill, *Chem. Soc. Rev.*, 2013, **42**, 2763.
4. Z. Cai, Y. J. Liu, J. Teng and X. Lu, *Acs Appl. Mater. Interfaces*, 2012, **4**, 5562.
5. P.-J. Demeyer, S. Vandendriessche, S. Van Cleuvenbergen, S. Carron, K. Bogaerts, T. N. Parac-Vogt, T. Verbiest and K. Clays, *ACS Appl. Mater. Interfaces*, 2014, **6**, 3870.
6. I. M. Krieger, F. M. O'Neill, *J. Am. Chem. Soc.*, 1968, **90**, 3114.
7. L. González-Urbina, K. Baert, B. Kolaric, J. Pérez-Moreno and K. Clays, *Chem. Rev.*, 2011, **112**, 2268.
8. C. F. Blanford, R. C. Schroden, M. Al-Daous and A. Stein, *Adv. Mater.*, 2001, **13**, 26.
9. Y. Takeoka, M. Watanabe, *Adv. Mater.*, 2003, **15**, 199.
10. Y. Yuan, Z. Li, Y. Liu, J. Gao, Z. Pan and Y. Liu, *Chem. Eur. J.*, 2012, **18**, 303.
11. E. Choi, Y. Choi, Y. H. P. Nejad, K. Shin and J. Park, *Sens. Actuators, B.*, 2013, **180**, 107.
12. H. Peng, S. Wang, Z. Zhang, H. Xiong, J. Li, L. Chen and Y. Li, *J. Agric. Food Chem.*, 2012, **60**, 1921.
13. X. B. Hu, G. T. Li, J. Huang, D. Zhang and Y. Qiu, *Adv. Mater.*, 2007, **19**, 4327.
14. J. Lee, Y. P. V. Braun, *Adv. Mater.*, 2003, **15**, 563.
15. J.-T. Zhang, L. Wang, D. N. Lamont, S. S. Velankar and S. A. Asher, *Angew. Chem. Int. Ed.*, 2012, **51**, 6117.
16. J.-T. Zhang, L. Wang, J. Luo, A. Tikhonov, N. Kornienko and S. A. Asher, *J. Am. Chem. Soc.* 2011, **133**, 9152.
17. C. E. Reese, S. A. Asher, *J. Colloid Interface Sci.*, 2002, **248**, 41.
18. A. Tikhonov, N. Kornienko, J.-T. Zhang, L. Wang and S. A. Asher, *J. Nanophotonics*, 2012, **6**, 063509.
19. M. Ben-Moshe, V. L. Alexeev and S. A. Asher, *Anal. Chem.*, 2006, **78**, 5149.
20. J. Shin, P. V. Braun and W. Lee, *Sens. Actuators, B.*, 2010, **150**, 183.
21. Y. J. Lee, S. A. Pruzinsky, and P. V. Braun, *Langmuir*, 2004, **20**, 3096.
22. S. Gehrke, *Adv. Polym. Sci.* 1993; **110**, 81.